Conference Paper, Published Version

Piano, Marco; Ward, Sophie; Robins, Peter; Neill, Simon; Lewis, Matt; Davies, Alan; Powell, Ben; Owen, Aled Wyn; Hashemi, Reza

Characterizing the tidal energy resource of the West Anglesey Demonstration Zone (UK), using TELEMAC-2D and field observations

Characterizing the tidal energy resource of the West Anglesey Demonstration Zone (UK), using TELEMAC-2D and field observations

Marco Piano, Sophie Ward, Peter Robins, Simon Neill, Matt Lewis, Alan G. Davies, Ben Powell, Aled Wyn Owen
Centre for Applied Marine Sciences (CAMS)
Bangor University, School of Ocean Sciences
Menai Bridge, UK
m.piano@bangor.ac.uk

M.Reza Hashemi
Department of Ocean Engineering and Oceanography
University of Rhode Island, Narragansett Bay Campus
Rhode Island, US

***Abstract* — A TELEMAC-2D hydrodynamic model has been applied to simulate high-resolution spatial distribution of currents in a proposed tidal stream demonstration zone. Complementary field observations provide both validation and vertical water column profile information at four sites across the region. We use the datasets to assess the theoretical power extractable from a generic tidal energy converter for deployments over the period of observation and compare these values to a typical average simulated month assessed over a 29.5 day lunar cycle. The results suggest that careful consideration should be given to micro-siting of devices within the zone as potential annual energy yield may increase by up to 180% between sites based on depth-averaged velocities of the undisturbed resource.**

I. INTRODUCTION

Strong tidal currents offer an apparent renewable and predictable resource from which we may extract energy to convert to electricity. However, the yield of a particular tidal energy converter (TEC) must be calculated relative to the overall energy cost, which includes deployment, maintenance and decommissioning. The yield will depend primarily on the resource available and the ability of a given device to convert that resource into electrical energy based on its characteristics [1]. Initial site assessments might focus on peak current flows, however attention should be given to the overall nature of the hydrodynamic resource as well as other practical constraints such as water depth, bathymetry, morphology and proximity to ports and grid infrastructure [2].

The Crown Estate (TCE), as manager of the UK seabed, announced plans in October 2013 to lease wave and tidal demonstration sites around the UK to encourage marine renewable technology developers to accelerate their efforts in UK waters. The West Anglesey Demonstration Zone (WADZ) in North Wales has been outlined for tidal stream energy development. TCE set out indicative guidelines in 2013 [3] for the principal requirements of demonstration zones - the criteria include having an appropriate energy resource, proximity to infrastructure, and the demand for opportunities to grow the marine sector. TCE constrained the resource criteria to include a mean spring peak velocity (V_{msp}) > 1.5 m s^{-1}, and a minimum water depth of 5 m (LAT).

For a tidal energy site to be considered desirable for commercial scale extraction, a number of key hydrodynamic criteria should be assessed, not least of these is the strength of the currents. However consideration should also be given to the direction of flow, as sites with rectilinear currents are generally more desirable for TEC devices, especially those without yaw capability. In this paper we use a TELEMAC-2D model to assess the WADZ region and consider the siting of a generic tidal stream energy converter at four sites where current measurements have been observed by seabed moored acoustic Doppler current profilers (ADCP). Most importantly, through this work we have significally improved the overall characterisation of the tidal energy resource for this region. Further, our assessment shows considerable spatial and temporal variability within the WADZ, suggesting that array leasing and device micro-siting requires careful consideration.

II. CASE STUDY

A. West Anglesey Demonstration Zone

The region to the west of Holy Island, Anglesey, UK (Fig. 1) has been selected for the TCE tidal stream demonstration zone project, due to strong currents experienced around this section of coast, over a relatively uniform water depth to seabed. The strong currents are created, for the most part, by a semi-diurnal Kelvin wave that propagates through the Irish Sea, generating large tidal ranges along the Welsh coast and strong tidal flows through restricted channels and around headlands and islands such as Anglesey. The WADZ can essentially be described as a headland with 'fixed' head differences in accordance with [4] The zone sea space covers an area of approximately 38 km^2, with a mean water depth of 38.4 m and V_{msp} is estimated by TCE to be 1.7 m s^{-1}. There is the potential for up to 100 MW of grid connected generating capacity [5]. Other sources estimate peak spring tide currents (V_{pk}) in excess of 2.5 m s^{-1} across large areas of the region [6] [7] [8]. Many of these studies are based on coarse resolution shelf scale models, or

analysis using a limited number of harmonic constituents with the potential for discrepancies and overestimation of the resource because energy flux within a site is related to the cube of the velocity and spatial variation will exist in flows over finer scales [7] [4]. Hence, validated high resolution regional models, simulated over a suitable time frame will provide better estimates.

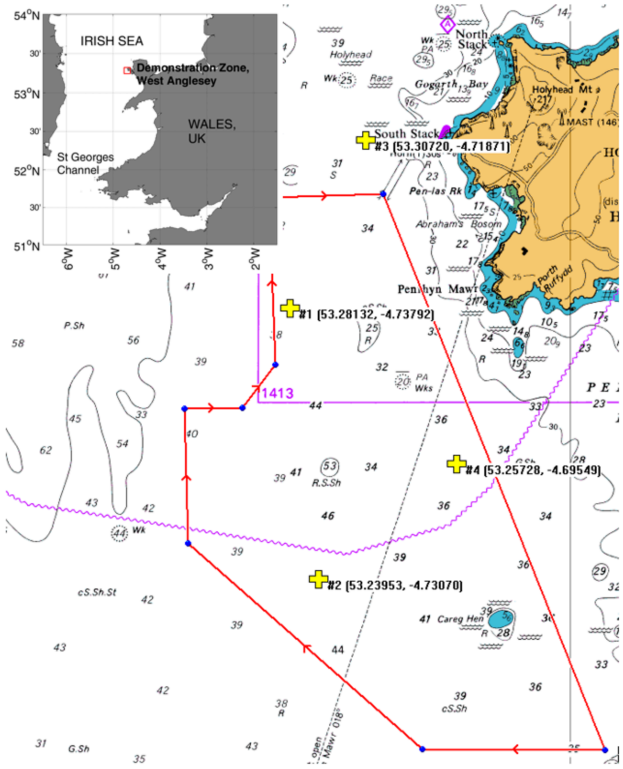

Figure 1. The region to the west of Holy Island, Anglesey with the area outlined for the tidal demonstrtion zone (red) and the position of four seabed moored ADCP stations (yellow crosses).

B. *Tides in the region*

Tidal stream currents are, in general, predictable throughout time, controlled by the movements of the earth-moon-sun system. However complexities exist when predicting currents, more so than for surface elevations, including variations in the vertical current profile as well as nonlinear and non-sinusoidal (asymmetric) behaviour in space and time: for example caused by wind-generated turbulence, eddy systems near complex bathymetry and steric or freshwater influence on density currents e.g. [2].

Tidal stream power patterns in the WADZ are dominated by a 25 h lunar day cycle created by the combination of the M_2 and S_2 semi-diurnal harmonic constituents, supplemented by smaller (diurnal and other) constituents such as O1 and P1. Some variation occurs between successive fortnightly cycles due to the influence of these smaller constituents (Fig. 2). Nevertheless, the monthly cycle of currents is relatively constant throughout the year.

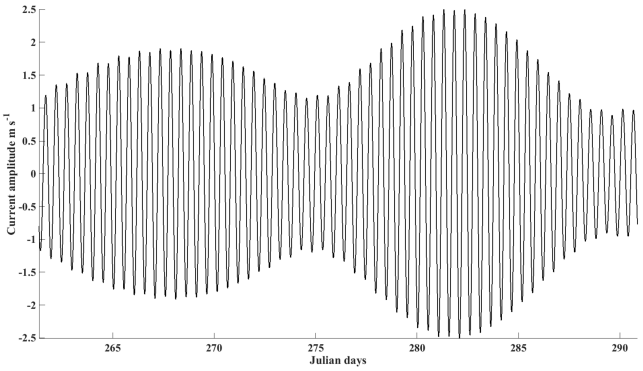

Figure 2. Amplitude and phase of depth-averaged tidal currents at ADCP station #1 in the WADZ (2014) for a complete lunar cycle as derived from five of the main harmonic constituents (M_2, S_2, N_2, O_1, K_1) using MATLAB T_TIDE analysis of observations.

C. *Site characterization*

In general, present horizontal-axis turbine technologies dictate that, for maximum rated power to be extracted, peak spring tidal velocities should exceed around 2.0 m s^{-1} in water depths of up to 50 m. However, this optimisation is driven by demand for sites that experience strong tidal flow, and severely limits the available sea space around the world where such technology can be economically deployed. Moreover, device operations in such extreme marine environments are difficult in practice, and wave-current interactions are also potentially significant (i.e., negatively affecting the available power). Present, forward-thinking research engages with the concept of lower-energy turbine optimisation, whereby available sea space is vastly increased, currents are rectilinear and less influenced by waves, and the environment is generally less harsh for engineering activity [7] [8].

The intensity of the hydrokinetic resource available for power conversion is proportional to the flow speed and for energy extraction this can be commonly defined in terms of the kinetic power (W) available, where the generated output from a turbine is calculated using:

$$P_{ki} = \frac{1}{2}\rho A \bar{U}^3 C_p \qquad (1)$$

where ρ is the density of seawater (1025 kg m^{-3}), $\bar{U}$ the depth-averaged flow velocity (m s^{-1}), A (m^2) is the swept area of the turbine blades upon which the flow acts and C_p is an overall coefficient of performance. In order to determine the best resource and likely generation rate from the turbine it is essential to understand the power available theoretically at any given location. Usually the kinetic power density available at a tidal energy site will be described in terms of its kinetic flux per unit area and an average value cited for site feasibility assessment studies. Here, we have defined this value as the average power density (W m^{-2}) that is output over the period of a complete lunar cycle (29.5 days),

which is the theoretical power available per unit area of the vertical water column:

$$APD = \frac{1}{2}\rho\frac{1}{n}\sum_{i=1}^{n}\bar{U}_i^{\,3} \quad (2)$$

In Eq. 2, i is the index of ensembled time increments $\bar{U}_i$ is the simulated velocity at that time step and n is the total number of time intervals (over a lunar cycle in this case). The economically viable threshold for potential site development will be determined by a number of factors.

III. Methodology

We have developed a high-resolution numerical ocean model for the entire Irish Sea, and applied it to simulate the tidal currents in the Anglesey region. In this way, the tidal stream resource has been assessed, including the spatial and temporal variability. The TELEMAC software suite has been used in previous studies to assess regional coastal environments at high spatial resolution [9] [10] [11]. This method of hydrodynamic characterization was chosen here due to its relative robustness when modelling near-shore locations and for its computational efficiency over large domains (i.e. using an unstructured grid to optimize resolution). *In-situ* measurements are presented of surface elevations from fixed tide gauges and tidal currents from moored ADCP stations, collected for this study. The measurements give an accurate assessment of the flow regime at particular times and enable the accuracy of the model to be validated.

A. Observations

Two Teledyne RDI sentinel V_{50} 500kHz, 5-beam ADCP instruments, fixed in trawl-proof, seabed mounted moorings were deployed concurrently in September 2014 and again in March 2015 at the locations shown in Fig. 1. The instruments were programmed with varying temporal resolution to capture both tidal and turbulent fluctuations. The ADCP measurements provide more than 60 days of data. The initial ADCP deployments (stations #1 and #2) were to the west of the WADZ and measurements were taken at turbulence frequencies (2 Hz) and tidal frequencies (0.067 Hz). Subsequent ADCP deployments were to the east (stations #3 and #4). A precision of <1 cm s^{-1} was achieved in all cases. These data were ensembled into 10 minute (#1, #3, #4) or hourly (#2) averages, with 0.6 m vertical resolution, for subsequent analyses and comparison against model outputs. Surface data affected by boundary layer interactions was omitted. Water depths at the deployment locations are approximately 30 - 40 m at lowest astronomical tide (LAT), with a mean tidal range of approximately 5.5 m.

B. Hydrodynamic Model

TELEMAC-2D (v6.3r2) is an open source, tidal model that solves the depth-averaged Saint-Venant free surface flow equations derived from the Navier-Stokes equations, for momentum and continuity [12]. A finite-element model grid has been applied to a domain encompassing the Irish Sea (approximate latitude 50°N to 56°N, longitude 8°W to 3°W, Fig. 3).

In regions where current velocities are high and bathymetry is shallow, the water column is vertically well mixed and therefore depth-averaged velocities can provide a good approximation of the flow characteristics. The vertical acceleration caused by pressure gradients due to the sloping seabed is small in the region around Anglesey, and therefore the hydrostatic assumptions of the model remain valid [10].

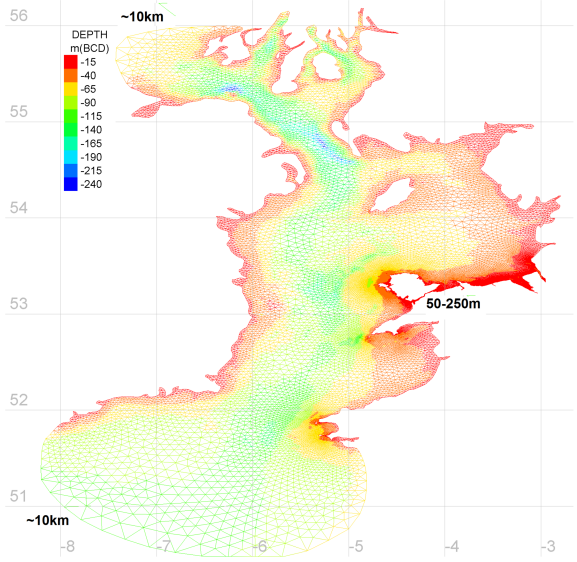

Figure 3. TELEMAC-2D Irish Sea model domain unstructured bathymetric mesh with depth profile given in metres below chart datum. Horizontal resolution at open boundaries and for the WADZ are indicated.

TELEMAC also uses an unstructured grid allowing the resolution of the mesh to be refined in areas of greater interest to the study. The mesh resolution is coarse (~10 km) at the model boundaries, increasing to 50 – 250 m around the Anglesey coast. The mesh is mapped onto gridded Admiralty Digimap bathymetry having horizontal resolution of approximately 30 m [13] and is corrected to mean sea level (MSL) using the UKHO VORF dataset [14]. TELEMAC-2D has the option of using tidal prediction boundary forcing [15]. We used the TPXO tidal database which contains up to 13 harmonic constituents (M_2, S_2, N_2, K_2, K_1, O_1, P_1, Q_1, M_4, MS_4, MN_4, M_f and M_m) on a structured grid of 0.25° resolution [16] [17]. TELEMAC utilizes both surface elevation change and the deduced horizontal component of current at the boundaries, interpolating between grid points where the mesh is less coarse. Note that only TPXO tidal forcing was applied to the model - additional forcing (e.g. wind, temperature, pressure) was omitted for this study, since astronomical tides dominate the current signal throughout the study region.

1) Simulations

The model was run for a 36 day period, discarding a 24 hour spin-up to provide 35 days of output. January 2014 was

chosen as a typical month in the year to run simulations, based on a comparison of mean predicted tide levels at Holyhead (2008 to 2026) from the British Oceanographic Data Centre (BODC) and monthly data values taken from the UK Hydrographic Office (UKHO) Admiralty Tide Tables (Table I).

TABLE I.

TIDAL RANGE PARAMETERS FOR HOLYHEAD

Values in metres above chart datum	*BODC (2008 - 2026)*	*ATT January 2014*
HAT	6.33	6.30
MHWS	5.66	5.60
MHWN	4.51	4.40
MLWN	2.02	2.00
MLWS	0.71	0.70
LAT	0.00	0.00

A water density of 1025 kg m^{-3} was used, wetting and drying of intertidal areas was included, as was the Coriolis effect. A simple approach was applied to model friction at the seabed across the whole domain using Chezy's law and a fixed friction coefficient value based on:

$$C = \frac{R^{1/6}}{n} = \frac{\left(\frac{zh}{2\sqrt{1+z^2}}\right)^{1/6}}{n} \quad (3)$$

where R is the hydraulic radius of the channel, in this case a triangular channel with approximate dimensions, 80 km wide (z) and 110 m deep (h) assuming that the largest channel into the domain has the greatest influence on dynamics, and n is the Manning roughness coefficient for a natural channel (0.030). The model time step was set at 10 s and graphical outputs were at 600 s intervals.

2) Validation

Simulated results are compared against *in-situ* observations for the amplitude and phase of the dominant harmonic constituents (M_2 and S_2) for surface elevation change at ten primary tide gauge stations and for currents using ADCP data from locations across the Irish Sea. The root mean square error (RMSE) of the model when compared with the observational data for amplitude and phase of M_2 and S_2 constituents are given in Fig. 4 together with the associated percentage variance scatter index. The normalised RMSE given by:

$$NRMSE = \frac{RMSE}{mean(obs)} \quad (4)$$

reveals a modelled error in M_2 surface elevation amplitude and phase of 4.3% and 0.9%, respectively. For S_2 the normalized errors are 6.5% (amplitude) and 2.0% (phase).

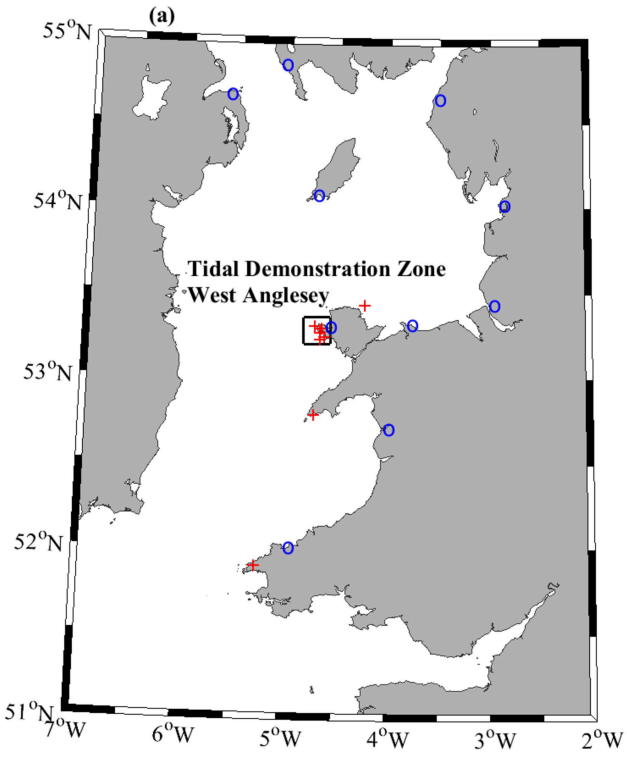

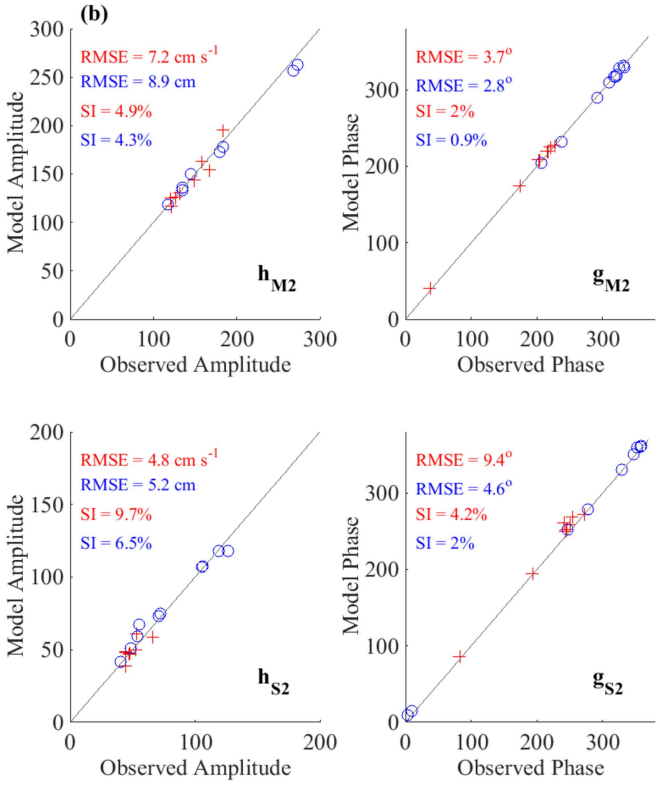

Figure 4. Map (a) indicates model validation positions of primary tide gauge stations (blue circles) for surface elevation and ADCP moorings (red crosses) for current amplitudes. Subplots (b) indicate regression analysis of amplitude, *h* and phase, *g* for M_2 and S_2 harmonic constituents derived from MATLAB T_TIDE analysis.

Similar evaluation for tidal currents reveals values of 4.9%, 2.0%, 9.7% and 4.2% respectively. Direct time series analysis of modelled velocity magnitude compared to depth-averaged observed ADCP data (Fig. 5) reveals good correlation between predicted and observed values for a 30 day time series which covers a complete lunar cycle over the duration of the observational deployment. Observed RMS current velocity (V_{rms}) for this analysis was 1.26 m s^{-1}, the simulated value for the same period was 1.29 m s^{-1}. Depth-averaged observational and modelled V_{pk} for this period were 2.52 m s^{-1} and 2.47 m s^{-1}, respectively. The extent to which flow magnitude measurements between predicted and actual regimes differs can be illustrated using regression analysis (Fig. 6), where an ideal one-to-one relationship would be identified by a line of best fit with an R^2 value equal to one. Any bias in the system is highlighted by a shift towards either the observed or predicted data. Here we see good correlation (R^2 = 0.92) between modelled values and observations with a slight over prediction by the TELEMAC-2D model.

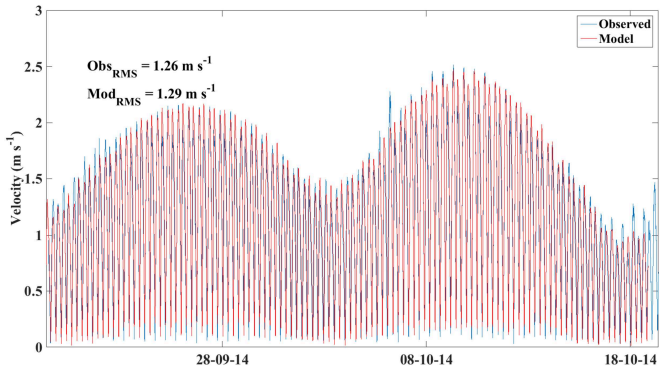

Figure 5. Simulated versus observed depth-averaged current speed for a complete lunar cycle at ADCP station #1.

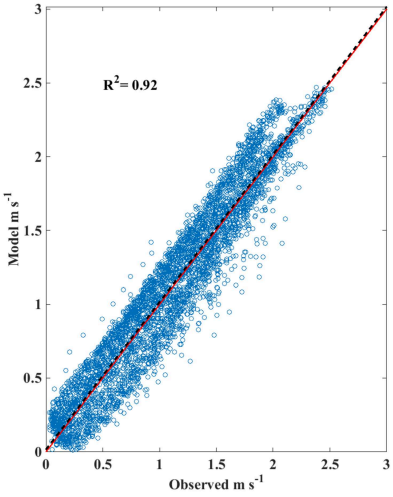

Figure 6. Regression analysis simulated versus observed current speed indicating correlation between the two datasets and any bias in the model. The red line indicates a perfect R^2 =1 fit, the black dashed line shows that 8% variance exists.

IV. RESULTS

Current speed and associated directionality, along with potential power density and annual theoretical energy yield available from the undisturbed raw resource at the four ADCP stations have been assessed and the results presented in Tables II and III.

A. *Variability of flow*

1) *Velocity magnitude*

The spatial distribution of currents is assessed using modelled outputs and plotted in Fig. 7 based on a complete lunar cycle. Significant variability across the WADZ and its surrounding area can be seen with a clear north – south divide. The strongest currents occur in the northeast close to headlands, where the tidal flow is constrained and enhanced. Mean (V_{avg}) and peak (V_{pk}) simulated velocities reach 1.6 and 3.7 m s^{-1}, respectively. For typical tidal conditions (i.e. based on M_2 and S_2 harmonics only) the flow reaches 3.1 (mean spring peak) and 1.7 m s^{-1} (mean neap peak). Across more than 50% of the WADZ V_{pk} exceeds a velocity of 2 m s^{-1}, while V_{msp} exceeds 1.7 m s^{-1}.

For micro-siting of devices to maximize potential power generation, it is important to understand where current velocities will exceed a specific threshold (e.g. device cut-in speed), and for what proportion of time this is achieved. In Fig. 8 the time that depth-averaged flow is in excess of 0.5, 1.0 and 2.0 m s^{-1} is plotted as a percentage of the total lunar cycle, with 25%, 50% and 75% exceedance times given as filled contours. Again the northeast region of the WADZ has the greatest potential for accessing highly energetic flows, which are sustained for longer periods of time.

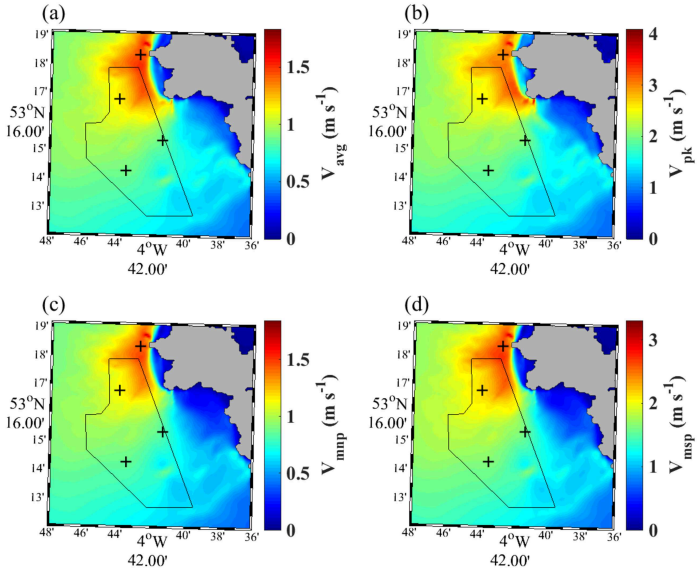

Figure 7. TELEMAC-2D simulated velocity magnitudes across the WADZ (black polygon). The four ADCP stations are marked as black crosses. A complete lunar cycle was assessed and mean (a), peak (b) mean neap peak (c) and mean spring peak (d) values are indicated.

2) Asymmetry and rectilinear misalignment

Peak current magnitude vectors (interpolated into an array of 100 vectors) are plotted in Fig. 9 (a) (as relative vector sizes), where the relative flood and ebb peak magnitude and direction from the four ADCP stations (Figs. 9 (b) to 9 (e)), show flood-dominance from station #1, #3 and #4, and ebb dominance otherwise. Even modest asymmetry between ebb and flood regimes leads to structural loading complexities, cavitation effects and cyclic loading of devices with stronger power generation occurring over one half of the tidal cycle [2] [18].

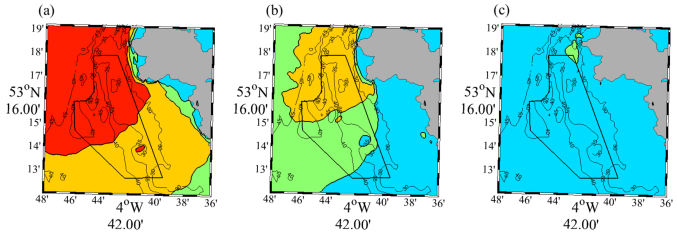

Figure 8. Contour plots indicating areas in the WADZ where time in excess of (a) 0.5 m s^{-1}, (b) 1 m s^{-1} and (c) 2 m s^{-1} occurs for >25% (green), >50% (yellow) and >75% (red) of a lunar cycle, 5 m depth contours are indicated.

Across the majority of the region, near-symmetrical, rectilinear flows exist, except in areas close to land where steep bathymetry and topographical changes combine to create turbulent eddy systems and misalignment in the ebb and flood direction. Rectilinear misalignment in ebb and flood direction in Table II is given by the absolute difference of peak direction values:

$$\theta_{assym} = \left| \left| \theta_{flood} - 180 \right| - \theta_{ebb} \right| \quad (5)$$

where a perfectly rectilinear tidal regime results in an asymmetry of zero degrees. No region contains truly rectilinear currents, however turbine performance and energy yield should be greatest where currents remain more rectilinear [19]. In agreement with the model, measured currents from the ADCPs that are further offshore are more rectilinear than those closer to shore.

3) Vertical distribution of velocity

Understanding the vertical structure of water column velocity is important for resource assessment of tidal stream sites and subsequently for placement of tidal stream devices [20]. Matching the turbine rotor position to the most effective flow conditions is key to optimising power extraction as power generated is ultimately derived from the cube of the current velocity (Eq. 1). Flow analysis of the water column at the four ADCP stations (Fig. 10 (a) to (d)) again reveals much higher flows to the north and particularly in the northeast, where near bed velocities can reach sustained flows of 2 m s^{-1} at station #3 during spring tides. Again we see evidence of ebb dominance at station #2 with higher velocities during the ebbing tide.

4) Undisturbed theoretical power extraction

A simple way to visualize the available power that can be extracted at a site is to plot velocity and power histograms that indicate the percentage of time that useful power may be generated over the total time of observation. Power density is calculated by applying a time series of velocity ensembles at a specified height above the seabed to Eq. 2 prior to any averaging. Here, we have considered two hub heights (15 and 25 m) at each ADCP station for comparison of vertical distribution of the resource. As indicated by Fig. 10 (f), the apparent power density at the most energetic site (station #3), reaches almost 14 kW m^{-2} at the higher hub position, where friction effects are weaker. Also power density values greater than 3 kW m^{-2} are sustained for longer periods than is the case further south and west.

Next we consider the placement of a generic TEC in the WADZ to assess the theoretical (undisturbed) resource available, using both modelled and observed velocities. This method provides the best approach as spatial variability in energetic tidal stream locations limits the extrapolation of currents to a few tens of metres. Therefore using spatially aggregated power density plots may not be viable for site feasibility studies [7] [21]. We apply depth-averaged velocities to simulate the power generated by a theoretical generic turbine having a rotor diameter of 16 m, a cut-in speed of 0.5 m s^{-1}, a rated speed of 2.0 m s^{-1} and an efficiency of 0.38 at cut-in, linearly increasing to 0.45 at rated output. The power curve generated by such a device is shown in Fig. 11 (a). Subsequent time series of theoretical output power at each ADCP station are shown in Figs. 11(b) to 11(e) and the performance of the TEC at each site is given in Table III. We see that time in excess of cut-in and rated speeds will increase when positioned to the north of the region and that annual energy yield potential will increase by up to 180% between sites based on observed calculations.

TABLE II.

CURRENT VELOCITY, EBB/FLOOD ASSYMETRY AND APD AT THE FOUR OBSERVATION STATIONS

	ADCP #1	***ADCP #2***	***ADCP #3***	***ADCP #4***
Mean velocity magnitude (m s^{-1})	1.11	0.91	1.35	0.87
Peak velocity magnitude (m s^{-1})	2.52	2.01	2.72	2.02
Mean spring peak velocity (m s^{-1})	2.11	1.78	2.46	1.61
Mean neap peak velocity (m s^{-1})	1.05	0.86	1.28	0.82
Θassym (deg)	6.90	1.02	12.32	4.70
Apparent power density (kW m^{-2})	1.32	0.75	2.16	0.61

TABLE III.

COMPARISON OF THE UNDISTURBED DEPTH-AVERAGED THEORETICALLY AVAILABLE RESOURCE ACROSS THE WADZ REGION

	TEC theoretical performance characteristics

	Observations				*Model*			
	#1	#2	#3	#4	#1	#2	#3	#4
Time cut-in speed exceeded (%)	81	75	85	74	80	72	84	76
Time rated speed exceeded (%)	7	<1	21	<1	10	<1	24	<1
Potential annual energy yield (GWh)	1.0	0.6	1.4	0.5	1.0	0.5	1.5	0.5

	TEC theoretical performance characteristics							
	Observations				*Model*			
Capacity factor (%)	29	17	43	14	31	15	46	15

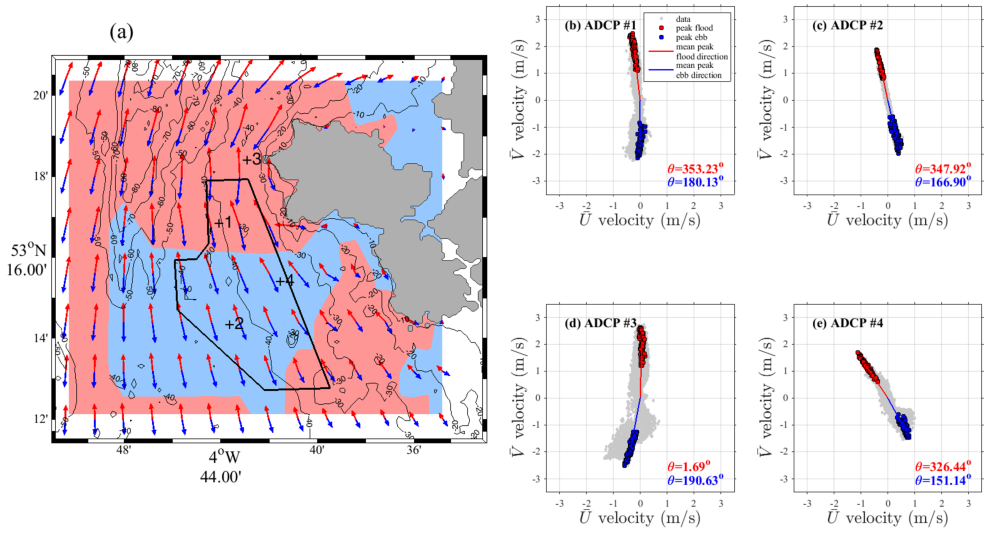

Figure 9. Simulated peak flood (red arrows) and ebb (blue arrows) flow magnitude and direction (a) with shaded areas indicating where relative flood or ebb dominance may occur. Subplots (b) to (e) show the depth averaged east and north velocity vector points (grey dots) for the four ADCP stations, with peak values highlighted accordingly and the subsequent incident angle of flow given by the mean peak values.

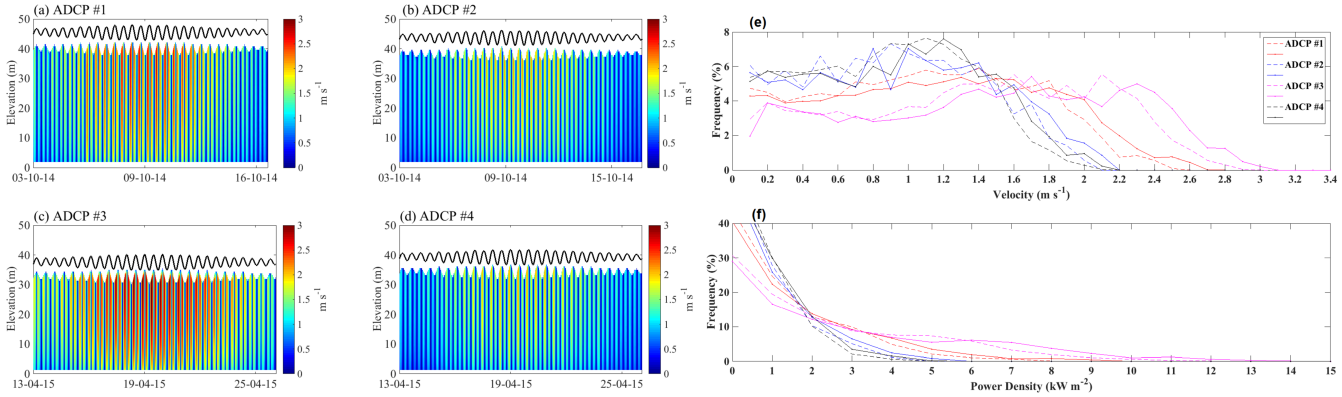

Figure 10. (a) to (d) ADCP station water column contour profiles of measured current speed interpolated between the 0.6 m vertical bin resolution and associated surface elevation change (black line) for the four ADCP stations. Surface bins (10%) have been excluded to remove side-lobe signal interference. Velocity (e) and kinetic power density (f) histograms showing occurrence as a percentage of a complete lunar cycle in 0.1 m s^{-1} and 1 kW m^{-2} bins for 15 m (dashed) and 25 m (solid) hub heights above the seabed at the four ADCP stations.

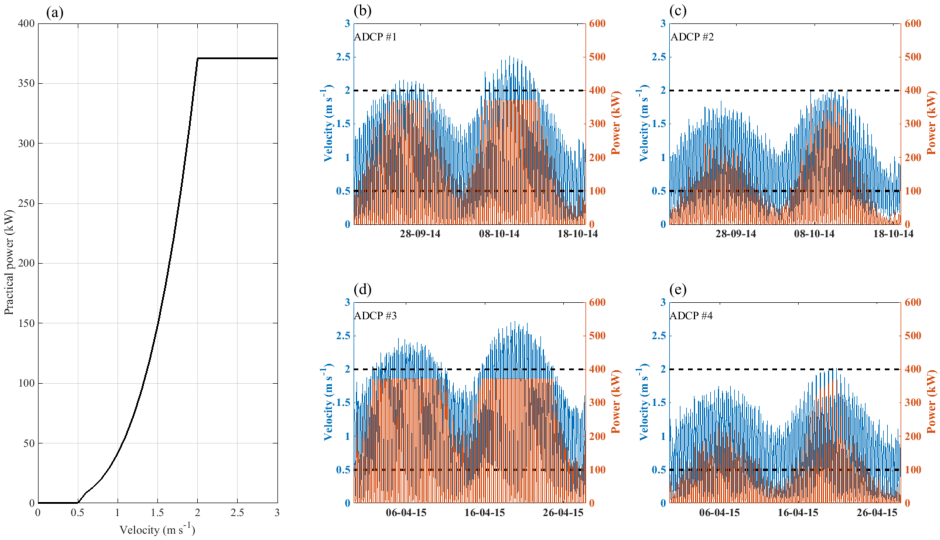

Figure 11. Generic TEC power output curve plot (a) and subsequent undisturbed power generation curves (orange) expected when depth averaged velocity (blue) from the four ADCP stations (b) to (e) is applied to the device. Dashed black lines indicate the cut-in and rated speed threshold of the device.

V. CONCLUSION

If tidal energy converters are to extract tidal energy efficiently, the resource should be assessed accurately using sophisticated models, in conjunction with *in-situ* measurements. Further the characteristics of the TEC should be tested for its suitability in the local hydrodynamic conditions. A multi-disciplinary approach to site characterisation should include an initial modelling assessment to predict, as accurately as possible, the likely spatial and temporal variation in the resource, followed by observational data collection in order to validate/calibrate the model, and to quantify the likely performance of the device under realistic conditions. High-resolution models (for example, <100 m for shelf-scale models) are desirable and these may require high performance computing (HPC) facilities that allow relatively low computational times for simulation. This is the approach that was utilised for this study.

This study reveals that areas to the north of the WADZ will yield greatest energy extraction potential, due to the higher velocities and consequent power density available. Such energetic conditions could increase loading stresses on devices, compared with calmer conditions further south. Initial site selection traditionally gives consideration to areas where the peak velocity is greatest and water depth suits the deployment of a given TEC. Consideration by developers looking to site their devices within the WADZ should also be given to the interaction of bathymetric, topographic and morphological features of the area, along with variability in the hydrodynamic regime over the year. For instance, peak flows may actually occur where asymmetric eddy systems develop, which could increase device loadings. Bottom substrate and its resultant friction coefficient will also be an important factor at the initial feasibility stage.

Although not considered here, the three-dimensional water velocity profile will vary where increased bed friction occurs and this will impact upon performance at lower hub heights. In highly energetic tidal streams, where the majority of the sea floor is bedrock, this consideration will be of lesser importance until device array deployments at a commercial scale dictate the necessity to expand to larger areas of seabed. Furthermore, surface gravity waves may propagate down the water column (wave-current interaction) and be an important factor in altering flow characteristics in these relatively shallow tidal stream regions. Further assessment of the resource should include uncertainty analysis that quantifies this interaction through coupled tide and wave modelling (preferably three-dimensional) and advanced observational techniques.

ACKNOWLEDGEMENT

This work was carried out as part of the Bangor University SEACAMS (Sustainable Expansion of the Applied Coastal and Marine Sectors) Project, part funded by the European Regional Development Fund (ERDF) by the Welsh European Funding Office (WEFO). The study formed part of a collaborative R&D project initiated by Dr Michael Roberts (SEACAMS R&D Project Manager) with the appointed WADZ third party management organization, Mentor Môn / Morlais. Data was kindly provided by the British Oceanographic Data Centre (BODC), United Kingdom Hydrographic Office (UKHO) and EDINA Marine Digimap Service.

VI. REFERENCES

VII.

[1] V. Ramos and G. Iglesias, “Performance assessment of Tidal Stream Turbines: A parametric approach,” *Energy Conversion and Management,* vol. 69, pp. 49-57, 2013.

[2] S. P. Neill, R. M. Hashemi and M. J. Lewis, “The role of tidal assymetry in characterizing the tidal energy resource of Orkney,” *Renewable Energy,* vol. 68, pp. 337-350, 2014.

[3] The Crown Estate, “UK wave and tidal key resource areas project,” 2013.

[4] Black and Veatch, “Phase II UK tidal stream energy resource assessment,” The Carbon Trust, London, 2005.

[5] The Crown Estate, “Summary report on wave and tidal demonstration zone identification process,” 2013.

[6] ABPMER, “WEBvision - Renewable (tide),” [Online]. Available: http://vision.abpmer.net/renewables/map_default.phtml?config=tide&resetsession=groups,resultlayers. [Accessed 08 May 2015].

[7] M. Lewis, S. P. Neill, P. E. Robins and M. R. Hashemi, “Resource

assessment for future generations of tidal-stream energy arrays," *Energy,* vol. 83, pp. 403 - 415, 2015.

[8] P. E. Robins, S. P. Neill, M. J. Lewis and S. L. Ward, "Characterising the spatial and temporal variability of the tidal-stream energy resource over the northwest European shelf seas," *Applied Energy,* vol. 147, pp. 510-522, 2015.

[9] C. Moulinec, C. Denis, C.-T. Pham, D. Rouge, J.-M. Hervouet, E. Razafindrakoto, R. W. Barber, D. R. Emerson and X.-J. Gu, "TELEMAC: An efficient hydrodynamics suite for massively parallel architectures," *Computers and Fluids,* vol. 51, pp. 30 - 34, 2011.

[10] P. E. Robins, S. P. Neill and M. J. Lewis, "Impact of tidal-stream arrays in relation to the natural variability of sedimentary processes," *Renewable Energy,* vol. 72, pp. 311 - 321, 2014.

[11] M. R. Hashemi, S. P. Neill, P. E. Robins, A. G. Davies and M. J. Lewis, "Effect of waves on the tidal energy resource at a planned tidal stream array," *Renewable Energy,* vol. 75, pp. 626 - 639, 2015.

[12] J. M. Hervouet, Hydrodynamics of free surface flows, John Wiley and Sons, 2007.

[13] EDINA, "Marine Digimap Service," [Online]. Available: http://digimap.edina.ac.uk. [Accessed 08 05 2015].

[14] United Kingdom Hydrographic Office, "VORF model VORF-UK08," UKHO, 2008.

[15] C.-T. Pham, "Use of tidal harmonic constants databases to force open boundary conditions in TELEMAC," in *XIXth TELEMAC-MASCARET User Conference*, Oxford, 2012.

[16] G. D. Egbert, A. F. Bennett and M. G. Foreman, "TOPEX/POSEIDON tides estimated using a global inverse model," *Journal of Geophysical Research,* vol. 99, no. C12, pp. 24821-24852, 1994.

[17] G. D. Egbert and S. Y. Erofeeva, "Efficient inverse modeling of barotropic ocean tides," *Journal of Atmospheric and Oceanic Technology,* vol. 19, pp. 183 - 204, 2002.

[18] S. Gooch, J. Thomson, B. Polagye and D. Meggitt, "Site characterization for Tidal Power," in *OCEANS 2009 Marine Technology for our future: Global and Local Challenges*, Biloxi, MS, 2009.

[19] S. F. Harding and I. G. Bryden, "Directionality in prospective Northern UK tidal current energy deployment sites," *Renewable Energy,* vol. 44, pp. 474-477, 2012.

[20] M. Lewis, S. Neill, P. Robins, S. Ward, M. Piano, M. Hashemi and A. Goward-Brown, "Observation of flow characteristics at potential tidal stream energy sites," in *EWTEC*, 2015.

[21] B. L. Polagye, J. Epler and J. Thomson, "Limits to the Predictability of Tidal Current Energy," in *Oceans 2010*, Seattle, 2010.